INTERNATIONAL JOURNAL FOR NUMERICAL METHODS IN FLUIDS
*Int. J. Numer. Meth. Fluids* 2011; **65**:812–833
Published online 22 December 2009 in Wiley Online Library (wileyonlinelibrary.com). DOI: 10.1002/fld.2215

# Cell face velocity alternatives in a structured colocated grid for the unsteady Navier–Stokes equations

A. Pascau*, †

*Área de Mecánica de Fluidos and LITEC, CSIC-Universidad de Zaragoza, Spain*

SUMMARY

The use of a colocated variable arrangement for the numerical solution of fluid flow is becoming more and more popular due to its coding simplicity. The inherent decoupling of the pressure and velocity fields in this arrangement can be handled via a special interpolation procedure for the calculation of the cell face velocity named pressure-weighted interpolation method (PWIM) (*AIAA J.* 1983; **21**(11):1525–1532). In this paper a discussion on the alternatives to extend PWIM to unsteady flows is presented along with a very simple criterion to ascertain if a given interpolation practice will produce steady results that are relaxation dependent or time step dependent. Following this criterion it will be shown that some prior schemes presented as time step independent are actually not, although by using special interpolations can be readily adapted to be. A systematic way of deriving different cell face velocity expressions will be presented and new formulae free of $\Delta t$ dependence will be derived. Several computational exercises will accompany the theoretical discussion to support our claims. Copyright © 2009 John Wiley & Sons, Ltd.

Received 20 October 2008; Revised 13 August 2009; Accepted 18 September 2009

KEY WORDS: CFD; colocated grid; unsteady flow

## 1. INTRODUCTION

It is well known that the arrangement of variables in a structured staggered grid produces a natural coupling between the velocity and pressure fields when a segregated approach is utilized. The $1\Delta$ discretization of the pressure gradient in the velocity equation, and viceversa, the discretization of the velocity divergence in the pressure (or pressure correction) equation is very effective damping the fluctuations that may arise in the iterative process because one variable responds naturally to the perturbations of the other. However, the coupling is not perfect and many times some sort of underrelaxation is required to prevent overflow. On the other hand, the colocated arrangement causes a decoupling between both fields, as a $2\Delta$ discretization arises in the continuity equation if no special interpolation is employed to calculate cell face velocities. In this sense the implementation of a staggered grid is more attractive as no additional care has to be taken to preserve a good PV coupling apart from underrelaxation. The ease of maintaining a stable velocity–pressure coupled iterative process is at the cost of making the coding more laborious since a different grid is required for each velocity component and for the pressure. If, to increase the convergence rate, a multigrid procedure is adopted, the whole implementation is prone to errors as the intergrid transfer operators

*Correspondence to: A. Pascau, Área de Mecánica de Fluidos, CPS Universidad de Zaragoza, María de Luna 3, 50018 Zaragoza, Spain.
†E-mail: pascau@unizar.es

Contract/grant sponsor: Spanish Ministry of Education; contract/grant numbers: CIT-370200-2005-6, ENE-2005-09214-204-03/ALT

are numerous and one has to write as many multigrid procedures as grids. Mainly due to this laborious multigrid coding there has been a growing tendency in the last two decades to use the colocated arrangement in which there is no multiplicity of prolongation or restriction interpolators.

Rhie and Chow showed how to deal with the PV coupling in a colocated arrangement in a seminal paper [1]. They put forward a special interpolation named pressure-weighted interpolation method (PWIM) that maintains the PV coupling by calculating convecting cell face velocities as the weighted mean of adjacent nodal values plus an extra term which is a function of the pressure field. In the first applications of the procedure in the Navier–Stokes equations, which require underrelaxation, it was observed that the final solution was dependent on the underrelaxation factor. Majumdar [2] and Miller and Schmidt [3] showed that the correct implementation involved the storage of the face velocity from iteration to iteration in the same manner as the nodal velocity is stored. To make the solution independent of the underrelaxation factor, as it should be, a new term arises that contains the difference between the convective flux and the weighted nodal mean, both at the previous iteration. One of the problems encountered with the PWIM approach is that the pressure field can produce cell face values that if plotted with resolved nodal values make the whole velocity field (nodes plus faces) look wiggly. This usually happens in regions where pressure gradient variations are significant. An interesting alternative based on a local solution was presented by Thiart [4] and slightly modified by Wang *et al.* [5] that reduces the oscillations at the cost of increasing the computational burden. Later, a rather close interpolation to PWIM named momentum-weighted interpolation method (MWIM) was proposed by Aksoy and Chen [6]. The only difference between both approaches lies in the quantity chosen to be interpolated, a complete term interpolation, PWIM, or a factor-in-term interpolation, MWIM. This minor difference produces very similar results with both approaches, both suffering from the same oscillation problems in the fields. A very thorough review of all work published with both techniques up to the end of 1997 is provided by Miettinen [7], although he considers MWIM to differ from PWIM in a manner that is not consistent with MWIM original paper.

The main problem of the colocated arrangement, in connection with what was mentioned in the previous paragraph, is that there are two different velocity fields: the convecting velocity at the cell face and the convected velocity at the cell center. The former does not possess a discretized equation of its own but instead is calculated as a function of the nodal values of the velocity and pressure. If the procedure is correctly implemented, the convecting velocity satisfies continuity within machine accuracy unlike the convected velocity that due to the pressure field does not. In the PWIM approach the continuity error for the nodal velocities is approximately proportional to the fourth derivative of the pressure field and to the cell size to the third power (or to the square of the cell size if the discretized terms are divided by the cell volume). Hence, in regions of large pressure variations a fine grid may be required to keep the mass imbalance for the cell center velocities below a certain tolerance.

The paper is mainly devoted to the discussion of cell face velocity alternatives for the (pseudo)unsteady Navier–Stokes equations. Its structure is as follows. We briefly describe the well-known Rhie and Chow interpolation in a steady case and its alternatives free of relaxation dependence. Then, the necessary changes for unsteady flow will be presented and several alternatives will be assessed, both new and old. Two sections are devoted to put forward the criterion to ascertain if a given scheme is time step dependent or not and to show how a non-consistent scheme can be converted into one free of $\Delta t$ dependence. Finally, some computational experiments will be shown to support our findings.

## 2. CELL FACE VELOCITY EXPRESSION. STEADY CASE

In order to introduce the new procedure, a short description of the east face velocity expression of a generic control volume associated with node $P$ will be explained in a steady case. The discussion will be short as details can be found elsewhere [3, 7]. Let $P$ and $E$ be the nodes that share the



DOI: 10.1002/fld

face $e$, all three along the $x$ coordinate, and $u$ be the velocity component along the same direction. The discretized momentum equation for $u_i$, $i=E,\ P$, is

$$u_i^*=\underbrace{\alpha_u\frac{\sum_{j|i}A_j^u u_j^*+S_i^u\Delta V_i}{A_{P|i}^u}}_{H_i^u}-\alpha_u\frac{\Delta V_i}{A_{P|i}^u}\left.\frac{\partial p}{\partial x}\right|_i+(1-\alpha_u)u_i^o \tag{1}$$

Subindices contain two letters when necessary: the first one refers to the category/localization of the factor and the second one refers to the equation node. For instance, $A_{P|i}^u$ would mean the diagonal coefficient of the $u_i$ equation, and $\sum_{j|i}$ would represent the sum over all neighbours of the node $i$. $S_i^u$ is the source per unit volume and the last term is the contribution from previous iteration. The fictitious equation for the velocity $u_e$ is the same on substituting $i$ by $e$. Rhie and Chow approach [1] can be interpreted as an interpolation that considers $H^u$ and $\Delta V/A^u$ to be piecewise linear functions between nodes and hence $H_e^u$ and $\Delta V_e/A_{P|e}^u$ are calculated as:

$$H_e^u=\overline{H_i^u}^e,\quad \frac{\Delta V_e}{A_{P|e}^u}=\overline{\left(\frac{\Delta V_i}{A_{P|i}^u}\right)}^e \tag{2}$$

The overline notation represents a mean, either arithmetic or harmonic [8], over the adjacent nodes that share the corresponding interface made explicit at the overline. By substituting $H_i^u$ of Equation (1), the face expression with arithmetic mean can be written as

$$u_e^*=\underbrace{\overline{u_i^*}^e}_{u_m}+\alpha_u\left(\underbrace{\overline{\left(\frac{\Delta V_i}{A_{P|i}^u}\left.\frac{\partial p}{\partial x}\right|_i\right)}^e-\frac{\Delta V_e}{A_{P|e}^u}\left.\frac{\partial p}{\partial x}\right|_e}_{u_c}\right)+(1-\alpha_u)\underbrace{[u_e^o-\overline{u_i^o}^e]}_{u_c^o} \tag{3}$$

$u_m$ is the mean over adjacent nodes and $u_c$ is the correction related to the pressure field that should be zero if the pressure gradient is constant [9]. This equation provides a solution independent of the underrelaxation factor. Majumdar [2] was the first to show the interpolation leading to Equation (3). The requirement that the contribution from the previous iteration should not be included in $H_e^u$ in order to have a solution independent of the relaxation factor was first observed by Miller and Schmidt [3] and later employed by others [10].

There are some alternatives to this PWIM interpolation. For instance, MWIM would interpolate the $H_e^u$ term in the following way:

$$\frac{A_{j|e}^u}{A_{P|e}^u}=\overline{\left(\frac{A_{j|i}^u}{A_{P|i}^u}\right)}^e,\quad u_{j|e}^*=\overline{u_{j|i}^*}^e,\quad \frac{S_e^u\Delta V_e}{A_{P|e}^u}=\overline{\left(\frac{S_i^u\Delta V_i}{A_{P|i}^u}\right)}^e \tag{4}$$

In Equation (3) we employ the velocities after momentum evaluation but this is not the sole option. We could also calculate $H_e^u=\overline{H_i^u}$ before the momentum equation is solved for. Xu and Zhang [11] compared PWIM in both formulations and showed that the one using the most recent values was always faster to converge. Its unsteady extension is the one we use throughout the paper.

The $u_e^*$ expression considers $H_e^u$ as the variable to be interpolated but an alternative expression can be derived if the interpolation is performed over $\sum_{j|e}A_j^u u_j^*+S_e^u$. In this case Equation (3) transforms into

$$u_e^*=\frac{1}{A_{P|e}^u}\overline{A_{P|i}^u u_i^*}^e+\alpha_u\frac{1}{A_{P|e}^u}\left(\overline{\Delta V_i\left.\frac{\partial p}{\partial x}\right|_i}^e-\Delta V_e\left.\frac{\partial p}{\partial x}\right|_e\right)+(1-\alpha_u)\left(u_e^o-\frac{1}{A_{P|e}^u}\overline{A_{P|i}^u u_i^o}^e\right) \tag{5}$$

Many researchers [12–14] employ a similar expression but others do not consider the ratio between the coefficients ($A_{P|i}^u$ and $A_{P|e}^u$) that comes about when performing a correct weighting procedure [15–19], that is, they employ the pressure term as in Equation (5) but the other terms are as in



DOI: 10.1002/fld

Equation (3). The amount of pressure dissipation is sometimes controlled by a coefficient (other than $\alpha_u$) that is adjusted *ad hoc* [15, 16, 20]. In the computational exercises to be presented with the unsteady version of this scheme we prefer to be consistent and stick to the correct expression given in Equation (5).

## 3. THE INTERFACE VELOCITY IN AN UNSTEADY FLOW

Let us consider now the case of an unsteady flow. We will present a new expression for $u_e^*$ and will relate it to previous ones in the literature. We will proceed in a similar fashion to the steady case by first writing the fictitious momentum equation at interface $e$ for a variable density case

$$A^u_{P|e}u^*_e=\sum_{j|e}A^u_j u^*_j+S^u_e\Delta V_e-\Delta V_e\left.\frac{\partial p}{\partial x}\right|^l_e+\frac{1-\alpha_u}{\alpha_u}\widetilde{A}^u_{P|e}(u^l_e-u^*_e)+\frac{\rho_e\Delta V_e}{\Delta t}(u^n_e-u^*_e) \tag{6}$$

with

$$\widetilde{A}^u_{P|e}=A^u_{P|e}+\frac{\rho_e\Delta V_e}{\Delta t},\quad A^u_{P|e}=\sum_{j|e}A^u_j \tag{7}$$

The most general case in which a (real or pseudo) time step can be combined with underrelaxation, that may also be interpreted as a local pseudotime step, will be described. By letting $\Delta t\to\infty$ the underrelaxed equation is obtained and if $\alpha_u$ is equal to one, time marching is used to seek the steady state. The equation is written in this way to quickly identify the meaning of the terms. The second to last term in the right-hand side is the contribution of the change in $u_e^*$ from (relaxed) iteration to (relaxed) iteration within a given time step, and the last term is the contribution of the unsteady change. The $u_e^l$ is the value at the previous inner iteration and $u_e^n$ is the value at the preceding time step. The algebraic equation is cast in this form because it becomes obvious that when there is no change in $u_e$, that is, $u_e^*=u_e^l=u_e^n$, it reduces to the discretized steady equation with no relaxation, hence, the final (steady) solution will not depend on either $\alpha_u$ or $\Delta t$. There has been much controversy over the years as to what is the expression for $u_e^*$ that is independent of these two parameters. Starting from this equation we will be able to derive a correct expression for $u_e^*$ and to spot the (sometimes subtle) errors in other expressions put forward by previous researchers. The equation for the node $P$ that shares interface $e$ is

$$A^u_{P|P}u^*_P=\sum_{j|P}A^u_j u^*_j+S^u_P\Delta V_P-\Delta V_P\left.\frac{\partial p}{\partial x}\right|^l_P+\frac{1-\alpha_u}{\alpha_u}\widetilde{A}^u_{P|P}(u^l_P-u^*_P)+\frac{\rho_P\Delta V_P}{\Delta t}(u^n_P-u^*_P) \tag{8}$$

Following the notation introduced before, the original Rhie–Chow interpolation assumes that

$$H^u_e=\frac{\sum_{j|e}A^u_j u^*_j+S^u_e\Delta V_e}{A^u_{P|e}}=\overline{\left(\frac{\sum_{j|i}A^u_j u^*_j+S^u_i\Delta V_i}{A^u_{P|i}}\right)}^e=\overline{H^u_i}^e \tag{9}$$

Following a parallel procedure to that leading to Equation (3) for $u_e^*$ provides

$$\begin{aligned}u^*_e=\overline{u^*_i}^e&+\overline{\frac{\Delta V_i}{A^u_{P|i}}\left.\frac{\partial p}{\partial x}\right|^l_i}^e-\frac{\Delta V_e}{A^u_{P|e}}\left.\frac{\partial p}{\partial x}\right|^l_e+\frac{1-\alpha_u}{\alpha_u}\frac{\widetilde{A}^u_{P|e}}{A^u_{P|e}}(u^l_e-u^*_e)-\overline{\frac{1-\alpha_u}{\alpha_u}\frac{\widetilde{A}^u_{P|i}}{A^u_{P|i}}(u^l_i-u^*_i)}^e\\&+\frac{\rho_e\Delta V_e}{\Delta t A^u_{P|e}}(u^n_e-u^*_e)-\overline{\frac{\rho_i\Delta V_i}{\Delta t A^u_{P|i}}(u^n_i-u^*_i)}^e\end{aligned} \tag{10}$$

This is not the equation to be implemented because $u_e^*$ is in both sides but written in this way one can grasp the independence of the final solution from both the underrelaxation factor and the time step. The first line on the RHS, that it is the only one remaining in the final solution, is the



DOI: 10.1002/fld

steady-state unrelaxed solution. Note that the $A^u_{P|i}$ factors in the pressure gradient do not contain the unsteady contribution, hence, when $u^*_e = u^l_e = u^n_e$ the final solution is the steady unrelaxed solution, as it should be. Reordering the equation one obtains

$$(1+\delta_e)u^*_e = \overline{(1+\delta_i)u^*_i}^e + \alpha_u \Delta t \left[ \overline{\frac{\delta_i}{\rho_i}\frac{\partial p}{\partial x}\bigg|_i^l}^e - \frac{\delta_e}{\rho_e}\frac{\partial p}{\partial x}\bigg|_e^l \right] + (1-\alpha_u)[(1+\delta_e)u^l_e - \overline{(1+\delta_i)u^l_i}^e]$$
$$+\alpha_u[\delta_e u^n_e - \overline{\delta_i u^n_i}^e] \tag{11}$$

with

$$\delta_{e,i} = \frac{\rho_{e,i}\Delta V_{e,i}}{\Delta t A^u_{P|e,i}} \tag{12}$$

which is the equation to be coded. This is the equivalent unsteady expression of the Rhie–Chow procedure. When $\Delta t \to \infty$, that is, $\delta_{e,i} \to 0$, the Rhie–Chow expression with Majumdar's correction, Equation (3), is recovered. This new expression bears strong resemblance to the one presented by Choi [21], but differs in some very important aspects that, unlike Choi's, make it truly independent of the time step. We named this cell face velocity evaluation as proper interpolation for a colocated treatment of the unsteady Reynolds-averaged equations (PICTURE) because we initially employed it in a (U)RANS code. There are some prior schemes in the literature whose formulation is very close to that just presented. Lai *et al.* [22] followed a similar approach by averaging the same term as PICTURE but they late adopted a series of simplifications that made the final expression move away from that of PICTURE. The actual $u^*_e$ equation they employed contains some unnecessary approximations that can produce a less accurate solution. Barton *et al.* [15] did not derive a special interpolation procedure for $u^*_e$, however, they eventually assemble a continuity equation for an unsteady problem that contains factors like $\Delta V_i / A^u_{P|i}$ and not $\Delta V_i / \widetilde{A}^u_{P|i}$. These coefficients multiply the pressure gradient correction in our continuity equation derived from Equation (10), hence, in that sense both schemes end up with a somehow similar continuity equation. The approach taken by Barton *et al.* is however so different that it cannot be considered a scheme close to PICTURE. Cubero and Fueyo [23] proposed a consistent scheme separating the temporal term from the underrelaxed one, i.e. they did not underrelax the complete $\widetilde{A}^u_{P|i} = A^u_{P|i} + \rho \Delta V_i / \Delta t$ but only $A^u_{P|i}$, whereas PICTURE works with the underrelaxed $\widetilde{A}^u_{P|i}$. Apart from this slight change both formulations are almost identical.

The writing of Equation (6) is not unique and another variant can lead to a different expression for $u^*_e$, in fact the one proposed by Choi. This non-uniqueness is due to the fact that at some point of the derivation one has to perform an averaging procedure equivalent to the Rhie–Chow proposal over a quantity that is dependent on the form of the starting equation. As the $u_e$ momentum equation is fictitious, the way we relate it to the actually solved $u_E$ and $u_P$ momentum equations is, to some extent, a matter of taste, something that will become clear further on. In this process of connecting terms of a fictitious equation with their counterparts in the ones solved, one important thing to care about is the independence of the steady solution from the time step. We will see that a seemingly correct interpolation, like Choi's, may induce time step dependency.

Let us write the fictitious $u_e$ momentum equation in a more traditional fashion

$$\frac{\widetilde{A}^u_{P|e}}{\alpha_u} u^*_e = \sum_{j|e} A^u_j u^*_j + S^u_e \Delta V_e - \Delta V_e \frac{\partial p}{\partial x}\bigg|_e^l + \frac{1-\alpha_u}{\alpha_u}\widetilde{A}^u_{P|e} u^l_e + \frac{\rho_e \Delta V_e}{\Delta t} u^n_e \tag{13}$$

and

$$u^*_e = \alpha_u \left[ \frac{\sum_{j|e} A^u_j u^*_j + S^u_e \Delta V_e}{\widetilde{A}^u_{P|e}} \right] - \alpha_u \frac{\Delta V_e}{\widetilde{A}^u_{P|e}} \frac{\partial p}{\partial x}\bigg|_e^l + (1-\alpha_u)u^l_e + \alpha_u \frac{\delta_e}{1+\delta_e} u^n_e \tag{14}$$



DOI: 10.1002/fld

The term in brackets is approximated as:

$$\frac{\sum_{j|e} A^u_j u^*_j + S^u_e \Delta V_e}{\widetilde{A}^u_{P|e}} = \overline{\left( \frac{\sum_{j|i} A^u_j u^*_j + S^u_i \Delta V_i}{\widetilde{A}^u_{P|i}} \right)}^e \tag{15}$$

The denominators of Equations (9) and (15) are different and the hypothesis of linear variation of the former does not take us to the same point as a similar hypothesis for the latter. The result will depend on the approach taken. Apparently both interpolations are correct[‡] as the only assumption involved in their derivation is the piecewise linearity of the interpolated functions between nodes. Nevertheless, we will show that the second one gives rise to an inconsistent steady solution unless special care is taken in the election of the interpolation operators. This problem did not arise in the steady relaxed equation because the difference between the denominators in the nonrelaxed and relaxed equations was a multiplicative constant for the whole field: $\alpha_u$. The case is different now.

Following the same path as before we end up with

$$u^*_e = \overline{u^*_i}^e + \alpha_u \Delta t \left[ \overline{\frac{\delta_i}{\rho_i(1+\delta_i)} \left.\frac{\partial p}{\partial x}\right|_i}^l - \frac{\delta_e}{\rho_e(1+\delta_e)} \left.\frac{\partial p}{\partial x}\right|_e^l \right] + (1-\alpha_u)[u^l_e - \overline{u^l_i}^e]$$
$$+ \alpha_u \left[ \frac{\delta_e}{1+\delta_e} u^n_e - \overline{\frac{\delta_i}{1+\delta_i} u^n_i}^e \right] \tag{16}$$

This is in fact the scheme proposed by Choi [21], who claimed that it was independent of the time step. The dividing function for Choi's scheme in Equation (15) is $\widetilde{A}^u_{P|e,i}$, whereas in PICTURE it is $A^u_{P|e,i}$, that is why every term in this equation is $1/(1+\delta)$ times the corresponding one in PICTURE. Observe that the asymptotic behaviour is correct, if $\Delta t \to \infty$ Rhie–Chow expression is obtained. The inconsistency of this scheme arises for small time steps and quickly worsens as the time step goes to zero. Yu *et al.* [14, 24] pointed out that this approach produced a steady-state solution that was $\Delta t$-dependent by showing the variation of the final value at monitoring points for different $\Delta t$ in a lid-driven cavity case. Their numerical findings were supported by an algebraic derivation which concluded that in fact Choi's scheme was time step dependent. Its assertion will be qualified in this work following a simpler theoretical analysis and will be underpinned by the computational evidence. Later we will show that Choi's extension to unsteady flows can be made time step independent with a judicious choice of the interpolation operator. We postpone a lengthier discussion on this issue to a next section, now we will explain another interpolation practice in which the assumption of piecewise linearity is taken over another quantity, $\sum_i A^u_i u^*_i + S^u$. In this case the equation obtained is

$$A^u_{P|e} u^*_e = \overline{A^u_{P|i} u^*_i}^e + \left[ \overline{\Delta V_i \left.\frac{\partial p}{\partial x}\right|_i}^l - \Delta V_e \left.\frac{\partial p}{\partial x}\right|_e^l \right] + \frac{1-\alpha_u}{\alpha_u} \widetilde{A}^u_{P|e}(u^l_e - u^*_e) - \frac{1-\alpha_u}{\alpha_u} \overline{\widetilde{A}^u_{P|i}(u^l_i - u^*_i)}^e$$
$$+ \frac{\rho_e \Delta V_e}{\Delta t}(u^n_e - u^*_e) - \overline{\frac{\rho_i \Delta V_i}{\Delta t}(u^n_i - u^*_i)}^e \tag{17}$$

which can be written in terms of $\delta$ and $A^u$ as:

$$A^u_{P|e}(1+\delta_e) u^*_e = \overline{A^u_{P|i}(1+\delta_i) u^*_i}^e + \alpha_u \left[ \overline{\Delta V_i \left.\frac{\partial p}{\partial x}\right|_i}^l - \Delta V_e \left.\frac{\partial p}{\partial x}\right|_e^l \right]$$
$$+ (1-\alpha_u)(A^u_{P|e}(1+\delta_e) u^l_e - \overline{A^u_{P|i}(1+\delta_i) u^l_i}^e) + \alpha_u (A^u_{P|e} \delta_e u^n_e - \overline{A^u_{P|i} \delta_i u^n_i}^e) \tag{18}$$

[‡]Not necessarily of equal accuracy.



DOI: 10.1002/fld

This is the form originally employed by Lien and Leschziner [25], Kadja *et al.* [12, 13] and Udaykumar *et al.* [26], and later claimed by Yu *et al.* [24] to be the only form that is unconditionally free of $\Delta t$-dependence. The new interpolation presented in Equation (11) also shares this property, something that will be demonstrated later. This form will be named in this paper as the undivided scheme (UNDS) because the averaged term is not divided by the $A^u_P$ coefficient. In all the derivations presented the source term, other than the pressure gradient and the contribution from previous values, is included in the term to be interpolated. In some instances, for example, when dealing with strongly buoyant flows, it may be convenient to treat it separately to obtain physically reasonable solutions [27–29], although other researchers have not found it necessary [7]. Also, when the pressure gradient and the source term have to be exactly compensated in both the cell volume and that of the face velocity an identical treatment is also required [30] and that implies keeping the source term in the same brackets as the pressure gradient.

It is worth mentioning that there have been other attempts to circumvent the problem of a non-unique solution linked to an inconsistent behaviour as the time step goes to zero or to infinity, as in Shen *et al.* [31, 32]. In these papers the authors included the contribution of the values of the previous time intervals in the $H_e$ interpolation when assembling the primary $u_e$ equation, something that is not correct. In the first paper they were more interested in getting rid of some wiggles in the solution and put forward another expression for $u_e$ (actually for the convective flux) that allowed them to obtain a smooth solution. Nevertheless, they still produced a time step dependent solution (however slight this dependency) as can be spotted in some of the figures in the paper. Its investigation is important in itself because it shows that sometimes another (undesirable) side effect of not carrying out a proper interpolation is the appearance of saw-tooth unphysical profiles. Yet, this is not a problem exclusive of inconsistent interpolations as some (smaller amplitude) wiggles can also appear in the solution with consistent interpolations, especially in regions of large pressure variations.

In the second paper [32] an alternative way of writing the $u_e$ equation is proposed. Its starting point is Equation (6) rewritten in the following manner:

$$\frac{\rho_e \Delta V_e}{\Delta t} u_e^* = \sum_{j|e} A_j^u u_j^* + S_e^u \Delta V_e - \Delta V_e \left.\frac{\partial p}{\partial x}\right|_e^l + \frac{1-\alpha_u}{\alpha_u} \widetilde{A}^u_{P|e}(u_e^l - u_e^*) + \frac{\rho_e \Delta V_e}{\Delta t} u_e^n - A^u_{P|e} u_e^* \tag{19}$$

which is adapted from the one in the paper to conform to our notation. Note that it is the temporal contribution what is kept in the LHS. Shen *et al.* presented this approach within a SIMPLEC procedure, although it can be derived with no specification of the PV coupling scheme adopted. Now the interpolation is realized over

$$\frac{\sum_{j|e} A_j^u u_j^* + S_e^u \Delta V_e}{\rho_e \Delta V_e} \Delta t = \Delta t \overline{\left( \frac{\sum_{j|i} A_j^u u_j^* + S_i^u \Delta V_i}{\rho_i \Delta V_i} \right)}^e \tag{20}$$

Shen *et al.* had to introduce a new $\beta$ factor to make it $\Delta t$ independent but here we will not pursue their approach, instead we will follow our procedure to see if we can obtain a proper $\Delta t$-independent scheme. After a little algebra the $u_e$ equation may be written as

$$\frac{1+\delta_e}{\delta_e} u_e^* = \overline{\frac{1+\delta_i}{\delta_i} u_i^*}^e + \alpha_u \Delta t \left[ \frac{1}{\rho_e} \left.\frac{\partial p}{\partial x}\right|_e^l - \overline{\frac{1}{\rho_i} \left.\frac{\partial p}{\partial x}\right|_i^l}^e \right] + (1-\alpha_u) \left[ \frac{1+\delta_e}{\delta_e} u_e^l - \overline{\frac{1+\delta_i}{\delta_i} u_i^l}^e \right]$$
$$+ \alpha_u (u_e^n - \overline{u_i^n}^e) \tag{21}$$

scheme that provides a final solution that is also independent of $\Delta t$. This scheme will be named PICTURE with a Tricky Weighted Operand (PICTURETWO). The tricky weighted operand refers to Equation (20). It is straightforward to show that this scheme is equivalent to UNDS if the cell volume is constant over the domain ($\Delta V_e = \Delta V_E = \Delta V_P$). Although this scheme will be shown to be only conditionally consistent, it will serve us as an example of how the criterion for unconditional $\Delta t$ independence proposed in this paper can detect other dependencies not inmediately obvious.



DOI: 10.1002/fld

If only the steady state is sought there is an extremely radical approach: to neglect all terms that represent the net changes from previous iterations in the $u_e^*$ expression, both relaxation-related and time-related. That amounts to only keeping the first two lines of the RHS of Equation (10) in which there is no contribution from previous values. By doing so the computational cost in terms of storage needs is reduced and no $\alpha_u$ and $\Delta t$ is present. This drastic simplification involves neglecting terms which can be of significance and hence the convergence deteriorates (or the procedure does not converge at all) in much the same way as when neglecting neighbour velocity corrections in SIMPLE-like procedures. Although its limitations, this approach has been followed by some researchers [16].

## 4. ALTERNATIVES FOR INTERPOLATING THE COEFFICIENTS

This section explores and discusses different alternatives for the calculation of the $\widetilde{A}^u_{P|e}$ coefficient. As mentioned previously, we consider a weighted arithmetic mean as the standard value, that is, $\widetilde{A}^u_{P|e}=\overline{\widetilde{A}^u_{P|i}}^e$. Let us consider the formal expression

$$\widetilde{A}^u_{P|e}=A^u_{P|e}+\frac{\rho_e\Delta V_e}{\Delta t}=A^u_{P|e}+\frac{\Delta M_e}{\Delta t} \tag{22}$$

$\Delta M_e$ being the mass contained in the $e$-volume. We can write

$$\overline{\widetilde{A}^u_{P|i}}^e=\overline{A^u_{P|i}}^e+\frac{\Delta M_e}{\Delta t} \tag{23}$$

Following Date [8] a weighted arithmetic mean with an $f_x$ geometric factor will be employed allowing for variable cell sizes. Developing the standard expression we have

$$\begin{aligned}\overline{\widetilde{A}^u_{P|i}}^e &= f_x\widetilde{A}^u_{P|P}+(1-f_x)\widetilde{A}^u_{P|E}\\ &= f_xA^u_{P|P}+(1-f_x)A^u_{P|E}+\frac{1}{\Delta t}(f_x\Delta M_P+(1-f_x)\Delta M_E)\end{aligned} \tag{24}$$

expression that is incompatible with Equation (23) as in general $\Delta M_e\neq f_x\Delta M_P+(1-f_x)\Delta M_E$, only it is true in a uniform grid. In fact, in a nonuniform grid the mass contained in the $e$-volume is $\Delta M_e=\widetilde{f_x}(\Delta M_P+\Delta M_E)$ with $\widetilde{f_x}$ equal $\frac{1}{2}$ only when the nodes are located in the center of their control volumes. Note that $f_x$ and $\widetilde{f_x}$ are different geometric factors. We will see the (bad) effects of inadequate averages in the results section, here we will not be pursuing this discussion further as there are additional hypotheses involved in the derivation of an interpolation *à la* Rhie–Chow as arguable (and perhaps as important) as this average. A thorough analysis on this issue may not be warranted and the preference for any interpolation has to be necessarily connected to its accuracy and consistency.

We have employed two different interpolation modes. The first one is the standard approach for $A^u_{P|e}$ and the $\widetilde{f_x}$-expression for $\Delta M_e$. This can be interpreted as an intensive practice for $A^u_{P|e}$ and a mass-consistent evaluation for $\Delta M_e$. The factor $\delta_e$ that appears in many of the formulae is calculated as:

$$\delta_e=\frac{\rho_e\Delta V_e}{\Delta t\,A^u_{P|e}}=\frac{\Delta M_e}{\Delta t\,A^u_{P|e}},\quad \widetilde{A}^u_{P|e}=(1+\delta_e)A^u_{P|e} \tag{25}$$

The second approach originates from the study carried out with the inconsistent schemes that is described in a following section. We interpolate the coefficient per unit mass in this way

$$\widetilde{A}^u_{P|e}=\left[\frac{A^u_{P|e}}{\rho_e\Delta V_e}+\frac{1}{\Delta t}\right]\rho_e\Delta V_e=\left[\overline{\left(\frac{A^u_{P|i}}{\Delta M_i}\right)}^e+\frac{1}{\Delta t}\right]\Delta M_e \tag{26}$$



DOI: 10.1002/fld

$\delta_e$ is calculated as $\delta_e=(\widetilde{A}^u_{P|e}/A^u_{P|e})-1$ and $\Delta M_e$ is calculated as before. This second approach will be shown to satisfy partly the interpolation required to make some schemes consistent, i.e. free of erroneous dependencies.

## 5. THE GOOD PRACTICE FOR THE INTERPOLATION OF THE VELOCITIES

The objective of this section is to show that there is a very simple criterion to ascertain if a given interpolation practice will unconditionally be time step independent. The criterion is stated as follows:

> 'If in the (steady state) limit when $u^*=u^l=u^n$ the expression for $u_e$ takes the same form as its corresponding steady equation, the scheme is time step independent'

This is a necessary and sufficient condition for a scheme to be $\Delta t$ independent. Evidently if some underrelaxation is incorporated the form should be that of the nonrelaxed steady equation. Once read the criterion appears rather trivial but surprisingly it is not always satisfied by some of the schemes proposed in the literature. Some adaptation might be required and we will discuss ways of making $\Delta t$-independent schemes that do not look as such at first sight. We will label schemes that satisfy the criterion with no required adaptation as 'unconditionally consistent'. We must note that the steady expression may also be dependent on the scheme. For instance, for UNDS is

$$A^u_{P|e}u^*_e=\overline{A^u_{P|i}u^*_i}^e+\left[\overline{\Delta V_i\left.\frac{\partial p}{\partial x}\right|_i}^e-\Delta V_e\left.\frac{\partial p}{\partial x}\right|_e\right] \tag{27}$$

but for PICTURE should be

$$u^*_e=\overline{u^*_i}^e+\left[\overline{\frac{\Delta V_i}{A^u_{P|i}}\left.\frac{\partial p}{\partial x}\right|_i}^e-\frac{\Delta V_e}{A^u_{P|e}}\left.\frac{\partial p}{\partial x}\right|_e\right] \tag{28}$$

UNDS is unconditionally consistent[§] and PICTURE also satisfies the criterion. However, if we rearrange Choi's scheme in the limit $u^*=u^l=u^n$ we end up with

$$u^*_e=\overline{\frac{1+\delta_e}{1+\delta_i}}^e u^*_i+\overline{\frac{1+\delta_e}{1+\delta_i}\frac{\Delta V_i}{A^u_{P|i}}\left.\frac{\partial p}{\partial x}\right|_i}^e-\frac{\Delta V_e}{A^u_{P|e}}\left.\frac{\partial p}{\partial x}\right|_e^l \tag{29}$$

and the factor $(1+\delta_e)/(1+\delta_i)$ makes the final solution to be time step dependent. The dependence is more evident for small time steps. Only in the limit $\Delta t\to\infty$ $(\delta_i,\delta_e\to 0)$ the scheme works well, but in that case we are not dealing with a true transient situation. The scheme, as will be explained in the next section, is conditionally consistent, meaning that it is imperative to use a certain interpolator to make it consistent.

This insatisfactory behaviour can be traced back to the denominator of the interpolation equation

$$\frac{\sum_{j|e}A^u_j u^*_j+S^u_e}{\widetilde{A}^u_{P|e}}=\overline{\left(\frac{\sum_{j|i}A^u_j u^*_j+S^u_i}{\widetilde{A}^u_{P|i}}\right)}^e \tag{30}$$

and more precisely to its time dependency, something that was not present in the first scheme. If there is any non-multiplicative $\Delta t$ factor in the term to be interpolated, the resultant scheme will be $\Delta t$ dependent. We define a multiplicative factor as a common factor that multiplies the whole term. $\widetilde{A}$ contains a non-multiplicative time factor whereas $A$ does not, and $\sum_{i|e}A^u_i u^*_i+S^u_e$ does not either. In the next section this assertion will be qualified because with a little extra work we can make *any scheme* free of unwanted $\Delta t$ dependence.

[§] In the results section we will show that this is completely true as long the $e$-volume is calculated in a certain way.



DOI: 10.1002/fld

PICTURETWO gives when $u^*=u^l=u^n$

$$u_e^*=\overline{\frac{\delta_e}{\delta_i}u_i^*}^e+\overline{\frac{\delta_e}{\delta_i}\frac{\Delta V_i}{A^u_{P|i}}\left.\frac{\partial p}{\partial x}\right|_i^l}^e-\frac{\Delta V_e}{A^u_{P|e}}\left.\frac{\partial p}{\partial x}\right|_e^l \tag{31}$$

The factor $\delta_e/\delta_i$ makes the solution inconsistent with the steady expression. However, this ratio does not contain any time factor because

$$\frac{\delta_e}{\delta_i}=\frac{\rho_e\Delta V_e}{\rho_i\Delta V_i}\frac{A^u_{P|i}}{A^u_{P|e}} \tag{32}$$

hence, the final solution will be independent of $\Delta t$. We can thus assure that in a general case the PICTURETWO solution will be independent of $\Delta t$ but dependent on the cell mass variation[¶] because Equation (31) can always be written as

$$A^u_{P|e}u_e^*=\overline{mr_iA^u_{P|i}u_i^*}^e+\left[\overline{mr_i\Delta V_i\left.\frac{\partial p}{\partial x}\right|_i^l}^e-\Delta V_e\left.\frac{\partial p}{\partial x}\right|_e^l\right] \tag{33}$$

$mr_i$ being the mass ratio, $(\rho_e\Delta V_e)/(\rho_i\Delta V_i)$. Compare this with Equation (27). Incidentally, this exemplifies the generality of the proposed criterion by which one can detect dependencies other than those on the time step not obvious in the first place.

## 6. A UNIFIED FORMULATION FOR ALL SCHEMES. HOW TO MAKE CONSISTENT AN OTHERWISE INCONSISTENT SCHEME

In this section a unification of all schemes will be described leading to interpolation criteria that will make both Choi's and PICTURETWO schemes free of erroneous dependencies. Let us start with the general equation for $u_e^*$ divided through by a generic function $\phi_e$. This function is specific of every scheme:

$$\frac{\widetilde{A}^u_{P|e}}{\alpha_u\phi_e}u_e^*=\frac{\sum_{j|e}A^u_ju_j^*+S^u_e\Delta V_e}{\phi_e}-\frac{\Delta V_e}{\phi_e}\left.\frac{\partial p}{\partial x}\right|_e^l+\frac{1-\alpha_u}{\alpha_u}\frac{\widetilde{A}^u_{P|e}u_e^l}{\phi_e}+\frac{\rho_e\Delta V_e}{\Delta t\phi_e}u_e^n \tag{34}$$

Similar equations can be written for $u_P^*$ and $u_E^*$. The arithmetic interpolation is realized over the first term on the RHS and the generic $u_e^*$ expression to be implemented is

$$\begin{aligned}\frac{\widetilde{A}^u_{P|e}}{\phi_e}u_e^*=&\overline{\widehat{\frac{\widetilde{A}^u_{P|i}}{\phi_i}u_i^*}}^e+\alpha_u\left[\overline{\widehat{\frac{\Delta V_i}{\phi_i}\left.\frac{\partial p}{\partial x}\right|_i^l}}^e-\frac{\Delta V_e}{\phi_e}\left.\frac{\partial p}{\partial x}\right|_e^l\right]\\&+(1-\alpha_u)\left(\frac{\widetilde{A}^u_{P|e}}{\phi_e}u_e^l-\overline{\widehat{\frac{\widetilde{A}^u_{P|i}}{\phi_i}u_i^l}}^e\right)+\alpha_u\left(\frac{\rho_e\Delta V_e}{\Delta t\phi_e}u_e^n-\overline{\widehat{\frac{\rho_i\Delta V_i}{\Delta t\phi_i}u_i^n}}^e\right)\end{aligned} \tag{35}$$

The four schemes are obtained if

$$\begin{aligned}&\phi_{e,i}=A^u_{P|e,i}\quad\text{PICTURE}\quad\phi_{e,i}=1\quad\text{UNDS}\\&\phi_{e,i}=\widetilde{A}^u_{P|e,i}\quad\text{Choi}\quad\phi_{e,i}=\frac{\rho_{e,i}\Delta V_{e,i}}{\Delta t}\quad\text{PICTURETWO}\end{aligned} \tag{36}$$

[¶]This is directly related to the expansion/contraction ratio of the grid in an incompressible case.



DOI: 10.1002/fld

Note that we do not preclude any average, that is, the widehat–overline can represent a geometric average or otherwise. As a matter of fact, to make the problematic schemes consistent we will have to resort to employing weighting factors other than geometric. We will discuss different alternatives to obtain a consistent steady solution and in order to do so we have to derive generic solutions when $u^*_{e,i}=u^l_{e,i}=u^n_{e,i}$. Operating with the previous equation it is easy to show that these are

$$\frac{A^u_{P|e}}{\phi_e}u^*_e=\widehat{\overline{\frac{A^u_{P|i}}{\phi_i}u^*_i}}^e+\left[\widehat{\overline{\frac{\Delta V_i}{\phi_i}\left.\frac{\partial p}{\partial x}\right|_i}}^{l^e}-\frac{\Delta V_e}{\phi_e}\left.\frac{\partial p}{\partial x}\right|^l_e\right] \tag{37}$$

We must remember that this final solution has to be equivalent to Equation (27) or Equation (28). It is inmediate to check that if one uses a geometric average both PICTURE and UNDS meet this requirement but Choi and PICTURETWO do not. The question we posit is: Is there any other average to be used in these schemes that leads to consistency? The answer is yes and we can find it by simple comparison with the consistent formulations. Let us take PICTURE for instance. Its steady-state expression is

$$u^*_e=\overline{u^*_i}^e+\left[\overline{\frac{\Delta V_i}{A^u_{P|i}}\left.\frac{\partial p}{\partial x}\right|_i}^{l^e}-\frac{\Delta V_e}{A^u_{P|e}}\left.\frac{\partial p}{\partial x}\right|^l_e\right] \tag{38}$$

Comparing this equation with Equation (37) it is realized that the average proposed should be one that satisfies

$$\widehat{\overline{\frac{A^u_{P|i}}{\phi_i}u^*_i}}^e\propto\overline{u^*_i}^e \tag{39}$$

because in that case the first term in the RHS of (37) will be the same as in PICTURE. The following average for a generic function $\zeta$ meets the requirement just mentioned

$$\widehat{\overline{\zeta_i}}^e=\overline{\frac{\phi_i}{A^u_{P|i}}\zeta_i}^e\Bigg/\overline{\left(\frac{\phi_i}{A^u_{P|i}}\right)}^e\Rightarrow\widehat{\overline{\zeta_i}}^e=\frac{\overline{(1+\delta_i)\zeta_i}^e}{\overline{(1+\delta_i)}^e}\quad\text{Choi}$$
$$\widehat{\overline{\zeta_i}}^e=\frac{\overline{\delta_i\zeta_i}^e}{\overline{\delta_i}^e}\quad\text{PICTURETWO} \tag{40}$$

the denominator is included to preserve the property that the average of a constant is the same constant. This average has as weighting factors for Choi and PICTURETWO

$$\widehat{f_x}=\frac{(1+\delta_P)f_x}{(1+\delta_P)f_x+(1+\delta_E)(1-f_x)},\quad\frac{\delta_P f_x}{\delta_P f_x+\delta_E(1-f_x)} \tag{41}$$

To be consistent with all $e$-located terms in the general $u^*_e$ expression of PICTURE the factors at $e$ have to be calculated as:

$$\frac{\phi_e}{A^u_{P|e}}=\overline{\left(\frac{\phi_i}{A^u_{P|i}}\right)}^e \tag{42}$$

For both Choi and PICTURETWO this reduces to $\delta_e=\overline{\delta_i}^e$. There is no other restriction. Observe that we can still use an arithmetic average for $A^u_{P|e}$ (if needed) but in that case for both schemes to be consistent $\widetilde{A}^u_{P|e}$ should be calculated as

$$\widetilde{A}^u_{P|e}=A^u_{P|e}(1+\delta_e)=\overline{A^u_{P|i}}^e(1+\overline{\delta_i}^e) \tag{43}$$



DOI: 10.1002/fld

and not with the traditional geometric average

$$\widetilde{A}^u_{P|e} = \overline{\widetilde{A}^u_{P|i}}^e \tag{44}$$

The work presented in this section was prompted by the fact that in some test cases with the inconsistent schemes we obtained solutions closer to the exact one when the second interpolation practice presented in a previous section was employed. When using the first interpolation mode the discrepancy was manifest, the results being quite far from the exact ones. In fact, according to Equation (42) the consistent PICTURE-equivalent interpolation for both is

$$\delta_e = \overline{\delta_i}^e \Rightarrow \frac{\Delta M_e}{A^u_{P|e}} = \overline{\left(\frac{\Delta M_i}{A^u_{P|i}}\right)}^e \tag{45}$$

Hence, we are obliged to average the coefficient per unit mass for the schemes to be consistent.[‖] That is why this interpolation resulted in a much better solution. We must stress again that these restrictions only apply to the inconsistent schemes. In principle, and in terms of consistency, any average is allowed for the $e$-located factors in PICTURE and almost anyone in UNDS. Incidentally, in the interpolations $\rho_e \Delta V_e$ may sometimes lose its mass-conserving expression in favour of being consistent. It is better to think of $\rho_e \Delta V_e$ as a variable with a required interpolation for consistency (as is $\widetilde{A}^u_{P|e}$) than to assign a real identity to such 'fictitious' variable.

It is convenient at this point to summarize the ideas discussed in this section. With traditional geometric averages the two inconsistent schemes will always produce solutions dependent either on the time step or on the spatial step. For consistency, i.e. the final solution independent of these steps, all widehat averages for generic terms $\zeta$ have to be averaged with Equation (40) to have a solution PICTURE-equivalent. Also, all $e$-factors contained in the $u^*_e$ general expression have to be calculated based on the restrictions given in Equation (42) depending on the specific function $\phi$. Of course, there is no point in using inconsistent schemes if later one seeks equivalent consistent expressions by choosing appropriate weighting factors, hence, this thorough discussion is only relevant to those who have already implemented inconsistent schemes and want to obtain correct results. There is an easy way out of the inconsistency: the interpolations and the weighting factors need to be changed. To this author's knowledge nobody has previously addressed the issue of the interpolation operators and their fundamental effect in the solution, at least with the inconsistent schemes.

All schemes will be compared in the next section in steady examples. Our intention is to utilize examples to support our claims and these are related to the good/bad use of pseudotime marching schemes with relaxation in problems moving toward steady state. Of course a scheme that produces steady solutions that are time step dependent cannot be recommended for unsteady problems so all comments in this paper are also relevant in unsteady situations.

## 7. RESULTS

All schemes will be applied to the solution of a simplified one-dimensional flow, which was employed formerly by Date [33] in a report on PV coupling in colocated grids. This flow, although simple, contains all the essential features of the pressure–velocity coupling and can highlight the

[‖]Strictly speaking, we used the arithmetic mean for the inverse which is the same as the harmonic mean in Equation (45).



DOI: 10.1002/fld

pros and cons of the approaches described. The continuity and Navier–Stokes equation to be discretized are

$$\begin{aligned} &\frac{\mathrm{d}}{\mathrm{d}x}\rho u = \dot{m} \\ &\frac{\mathrm{d}}{\mathrm{d}x}\rho u^2 = -\frac{\mathrm{d}p}{\mathrm{d}x} + \dot{m}u + \mu\frac{\mathrm{d}^2u}{\mathrm{d}x^2} + S_m \end{aligned} \tag{46}$$

These equations govern the motion of an incompressible 1D flow with mass and momentum injection. $\rho$ may be considered as a line density (kg/m) and $\dot{m}$ represents the mass source (kg/m/s injected to or extracted from the 1D domain), which may depend on $x$ and/or $t$. In the Navier–Stokes equation, the momentum source is $\dot{m}u$ as each kg/m/s of fluid injected/extracted at one point has to bring in/take away $\dot{m}u$ momentum units per meter and per second, otherwise the variable $u$ would have two different values at the same point. $S_m$ represents additional momentum sources due to gravity forces and other body forces in non-inertial reference frames, if any. By adjusting appropriately the source terms a wealth of different (continuous and discontinuous) analytic solutions may be obtained that will allow us to compare the different unsteady interpolations. All physical properties have been taken as constants of value one and the inlet conditions are $u_o = 1$ and $p_o = 0$.

We will show cases where the inconsistency is revealed and where the changes brought about by consistent interpolations are more noticeable. The three cases tested correspond to different mass and momentum source functions. There is no special reason behind the use of this concrete blend of sources but the fact that they have been employed, among others, as computational exercises in a CFD course taught by the author. Arguably, these cases are neither computationally demanding (good) nor numerically demanding (not that good), except perhaps the first case because of the discontinuity in the pressure field. However, the main purpose of this section is just to support the theoretical findings which form the core of the paper and these examples provide clear answers to the questions raised in this work. To show that a scheme is $\Delta t$ or $\Delta V$ dependent can perfectly be realized in rather simple one-dimensional flows as the ones picked up. If there are any doubts cast on whether a consistent scheme in 1D will remain so in 2D or 3D problems, we must point out that the cell face velocities in a colocated grid are always calculated averaging the nodal values situated only along one coordinate which is perpendicular to the face. The cell face velocity is always calculated as if the problem was 1D. Thus, from the point of view of PWIM interpolation one could say that 3D problems are $1+1+1$D.

The first test contains a constant mass and momentum source in the interval $(0.3, 0.7)$ of a unity domain. The second one has only a linear momentum source in the same interval and the third one is chosen to highlight some problems that can arise when using UNDS. The exact solutions for the cases tested are given in the Appendix. The computational results are always corresponding to a fully converged solution. If nothing is specified that means a residual below $10^{-14}$ for the mass imbalance and below $10^{-12}$ for the velocity equation, both in the energy norm. They are calculated as follows:

$$\begin{aligned} \text{massres} &= \sqrt{\sum_P \left|(\rho u_{e|P} - \rho u_{o|P}) - \dot{m}\Delta x\right|^2} \\ \text{velres} &= \sqrt{\sum_P \left|\frac{A^u_{P|P}u_P - \sum_{j|P} A^u_j u_j - S^u_P - GF^u(P_{w|P} - P_{e|P})}{A^u_{P|P}u_P}\right|^2} \end{aligned} \tag{47}$$

In $S^u_P$ the contribution of the previous iteration and the preceding time step is not considered. In all figures the exact solution is shown as a solid line. The values at nodes and faces will be portrayed.

In Figure 1 the pressure distribution in the first case for several approaches is depicted. This case was one where the time dependency of Choi's scheme was evident. The grid points are distributed with the idea of combining uniform regions with others having a relatively rapid variation of the contraction/expansion ($c/e$) ratio. We found that in regions of rapid variation of the $c/e$ ratio the



DOI: 10.1002/fld

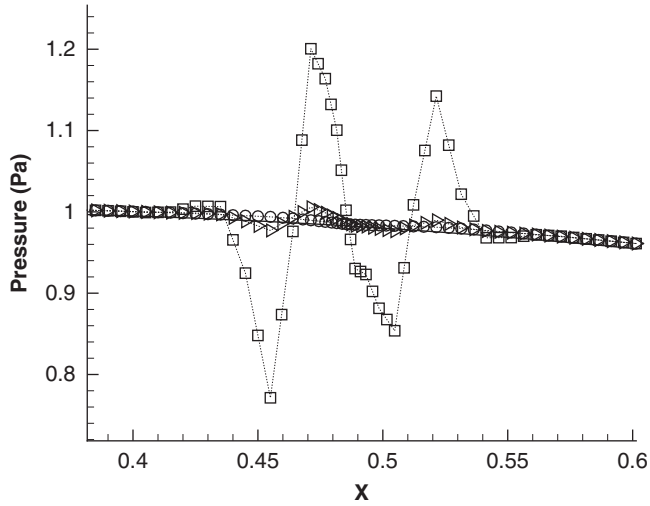


Figure 1. Pressure distribution for the first case with Choi's scheme. □ Choi inconsistent approach $\Delta t = 10^{-4}$; ▷ Choi inconsistent approach $\Delta t = 5.\ 10^{-4}$; ○ Choi approach consistent with PICTURE.

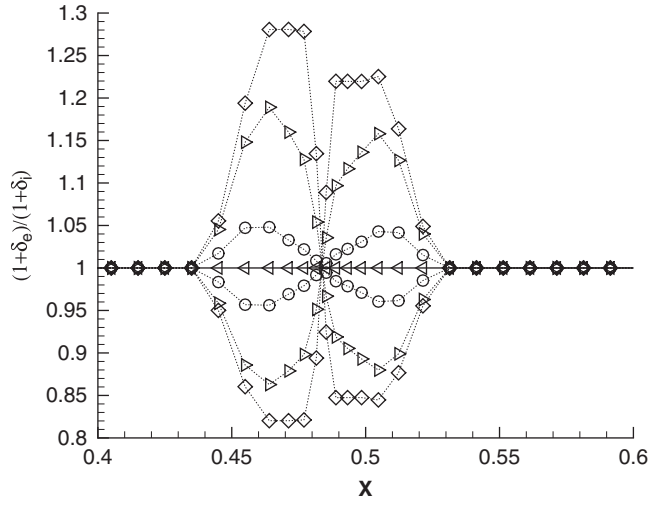


Figure 2. Factors dependence on $\Delta t$. ◁ $\Delta t = 10^{+5}$; ○ $\Delta t = 10^{-4}$; ▷ $\Delta t = 10^{-5}$; ◇ $\Delta t = 10^{-10}$.

inconsistencies were more noticeable. There are 45 volumes of uniform size $\Delta x = 0.01$, 5 volumes with a contraction ratio of 0.8 (the first one with $\Delta x = 0.01$), 6 volumes with an expansion ratio of 1.2 (the first one with $\Delta x = 0.0033$) and again a constant zone with $\Delta x = 0.01$. These ratios are in the limit of the recommended values for not losing accuracy in the discretization. Only the region of nonuniform spacing is presented. As we mentioned previously the inconsistency for Choi's scheme is more revealing as the time step is reduced. With $\Delta t = 5 \times 10^{-4}$ the oscillations are pretty noticeable but they have increased dramatically for $\Delta t = 10^{-4}$. In the figure, the solution of the modified Choi's approach, consistent with PICTURE and identical to it, is also shown. The oscillations are absent in this case and the solution lies very near the exact solution given by the solid line.

To understand why the effect of the inconsistency is more noticeable when $\Delta t$ is of order $10^{-4}$ or below, Figure 2 shows the evolution of $(1+\delta_e)/(1+\delta_i), i = E, P$, for four different $\Delta t$: $10^{+5}$, $10^{-4}$, $10^{-5}$ and $10^{-10}$, $\delta_e$ being calculated as $\overline{\delta_i}^e$. There are two factors associated with the same interface and for a given $\Delta t$ they are drawn in the figure as two lines with the same symbol. For a strict equivalence to PICTURE these factors should be 1 and they have in fact this value when



DOI: 10.1002/fld

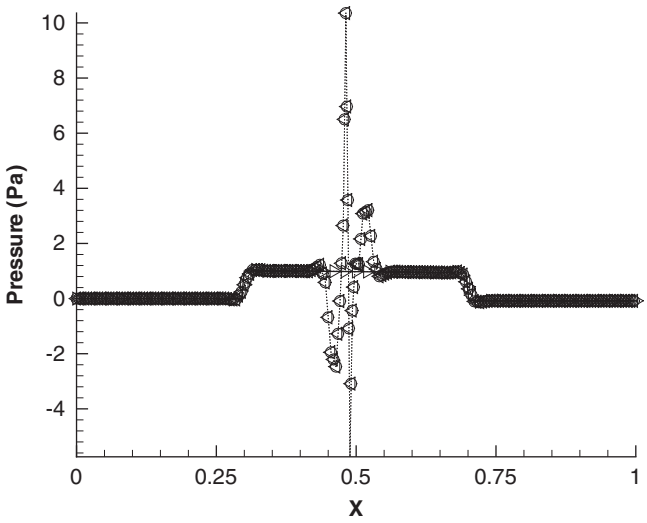


Figure 3. Pressure distribution with PICTURETWO. ▷ PICTURETWO consistent with PICTURE; ∘ PICTURETWO inconsistent, $\Delta t = 10^{+5}$; ◁ PICTURETWO inconsistent, $\Delta t = 10^{-5}$.

the time step is $10^{+5}$, giving in that case a very smooth solution. As can be seen diminishing $\Delta t$ separates them more and more from unity.

There is a direct link between this separation and the quality of the result: the more the distance exists the more amplified the oscillations appear as these nonunity factors become dominant in the averaging process, vitiating the final solution. In the limit $\Delta t \to 0$ the factors are $\delta_e/\delta_i$. Let us remember that these are the ratios appearing in the inconsistent PICTURETWO. Hence, as a conclusion in this case, the oscillations produced by Choi's approach are of smaller or equal amplitude than those produced by PICTURETWO for all time steps. The PICTURETWO results, shown in Figure 3, corroborate this assertion as large amplitude oscillations are present. The complete unity domain is drawn to see the overall behaviour. The two solutions for different $\Delta t$ are the same, as expected, and the solution consistent with PICTURE is exactly the same as that of Choi's approach consistent with PICTURE.

In a true transient case it can be shown that $\delta$ is related to the inverse of the local CFL number (convective plus diffusive). In the case $\Delta t = 5 \times 10^{-4}$, both $\delta$ and CFL are of order unity in most of the domain, the former decreasing significantly in the nonuniform part. There are two combined causes for the appearance of oscillations in Choi's scheme: small $\Delta t$ and significant variation of $\Delta V/A^u$. The combination of both makes $\delta$ become significant against unity with considerable changes in some regions and this causes the factors to move away from unity. To highlight the necessity of both acting at the same time let us mention that we have obtained with Choi's inconsistent formulation a perfectly smooth solution for any $\Delta t$ (any CFL) in a uniform grid where $\Delta V/A^u_P$ hardly changed. The oscillations may appear if $\delta$ changes quickly in a significant manner, provided $\delta$ is not negligible compared with one. The cause may be a rapid variation of $c/e$ ratio as in this case but it may well be quite another reason in a different problem. The oscillations will appear for CFL number roughly of order one, yet we must make clear that these oscillations have nothing to do with the stability of the explicit time integration as the usual CFL condition has. In Figure 4 the velocity is shown for the same case in the region of quick variation of $c/e$ ratio. The solution for Choi's inconsistent approach with $\Delta t = 10^{-4}$ is very close to the exact one, fact that highlights a systematic finding in this work: in all the cases studied the inconsistency is always more reflected in the pressure than in the velocity, where is hardly noticeable sometimes. This statement is not intended to be general but it is important as Choi [21] and Yu *et al.* [14, 24] compared only velocities and not pressure. Finding tiny variations in the former does not necessarily mean that the scheme is time step independent. Both variables have to be checked for time step independence. In Shen *et al.* [31] the lines where the dependency can be spotted are the isobars.



DOI: 10.1002/fld

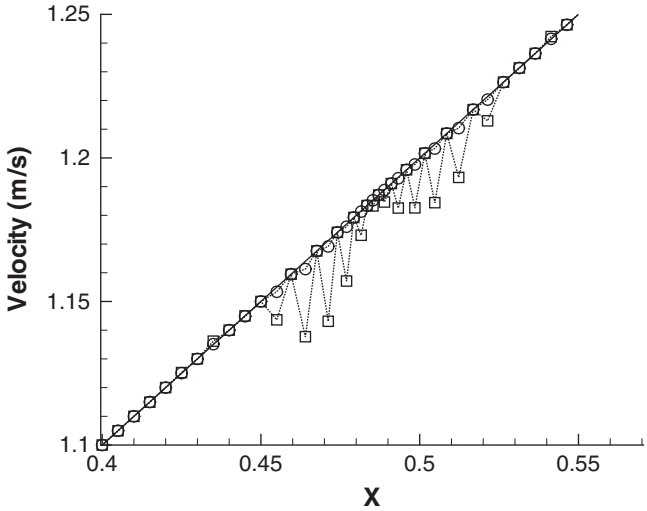


Figure 4. Velocity distribution in the first case. ∘ Choi inconsistent, $\Delta t = 10^{-4}$; □ Choi inconsistent, $\Delta t = 10^{-5}$.

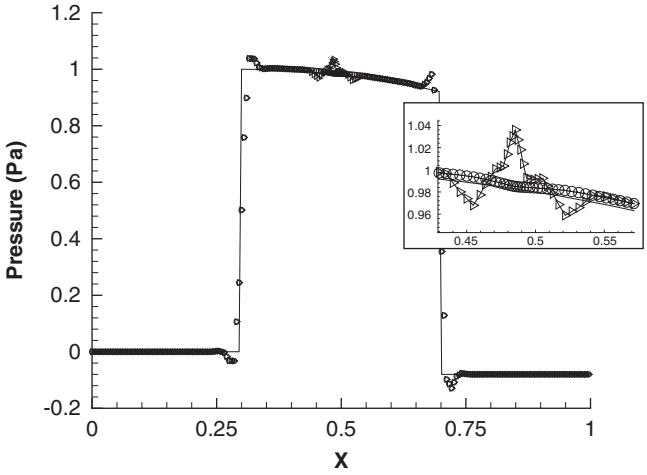


Figure 5. Pressure distribution for the first case with the two consistent schemes. ∘ PICTURE; ▷ UNDS.

There are some situations where UNDS shows oscillations although it is a consistent scheme. This case is one of them and it has to do with the initial assumption made in the scheme derivation. Let us remind that PICTURE assumes that $(\sum_i A_i^u u_i^* + S^u)/A^u$ is linear, whereas UNDS makes the same assumption for $\sum_i A_i^u u_i^* + S^u$. The oscillations can be directly related to the linearity of this term (or the lack thereof). In Figure 5 the solution with both schemes is presented with an inset for details and in Figure 6 the term supposed to be linear is depicted. Over most part of the domain both solutions are indistinguishable but in the nonuniform region UNDS result is much worse. It is obvious that UNDS incorrectly assumes that $\sum_i A_i^u u_i^* + S^u$ is linear and this false assumption produces the oscillations in the nonlinear region. The local maxima and minima in the solution are related to intervals where the second derivative of the addend is large in relative terms. On the other hand, PICTURE assumption is correct over the whole domain resulting in a smooth solution. It was mentioned in a previous section that there are consistent schemes that can produce oscillations, now it is understood that these are partially linked to the adequacy of the linearity assumption implicit in the derivation of the cell face velocity. There might be other required interpolations that can affect the amplitude of the oscillations, if any.



DOI: 10.1002/fld

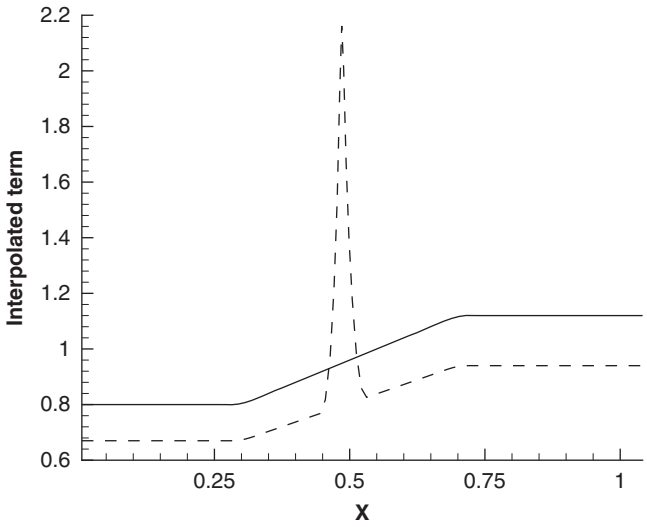


Figure 6. Interpolated term in the first case. Solid line $(\sum_{j|i} A^u_j u^*_j + S^u_i)/A^u_{P|i}$. Dashed line $\sum_{j|i} A^u_j u^*_j + S^u_i$.

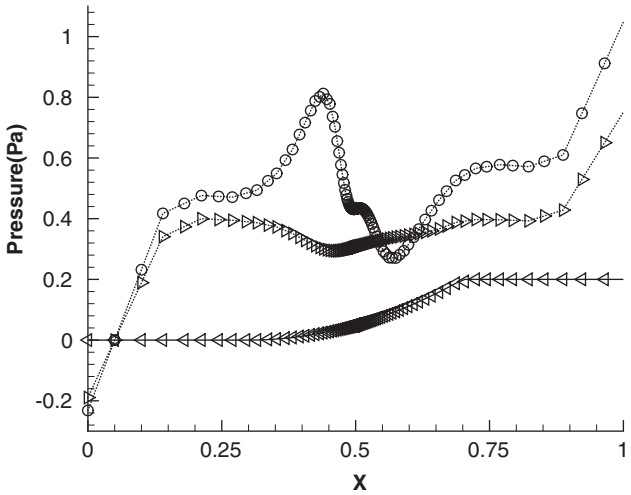


Figure 7. Pressure for the second case. ∘ Choi inconsistent $\Delta t = 10^{-4}$; ▷ Choi inconsistent $\Delta t = 10^{-3}$; ◁ Choi inconsistent $\Delta t = 10^{+5}$.

The second case presented in Figure 7 also reveals the inconsistency of Choi's scheme. This is a case for which the solution is very smooth but the grid adopted has rapid variations in the cell size, $\Delta V$, in order to produce large changes in $\delta$. The grid is contracting with a contraction ratio of 0.8 up to $x = 0.5$ and then expanding with an expansion ratio of 1.2 until $x = 1$. The scheme is run with different $\Delta t$: $10^{-4}$, $10^{-3}$ and $10^{+5}$. The solutions with the first two $\Delta t$ are a complete nonsense, neither the tendency nor the values are reproduced. The solution for $\Delta t = 10^{+5}$, in which $\delta$ is very small compared with one, lies on top of the exact solution as does the consistent alternative for any $\Delta t$ (not shown). A companion figure is Figure 8 where the PICTURETWO results with $\Delta t = 10^{-4}, 10^{+5}$ are presented along with the solution obtained with PICTURETWO consistent with PICTURE. Again, the solutions of the inconsistent scheme, identical for both $\Delta t$, are far off the exact one. Near 0.5 there are a great many points lying outside the $y$ axis range as the actual pressure range of the solution goes from $-10000$ to 15000. Apparently the effect of the ratio change at 0.5 gives rise to huge oscillations near this point and vitiates the solution all over the domain. Let us remember that PICTURETWO is unduly dependent on the finite volume size variation. To check the theoretical finding of independence of PICTURETWO from $\Delta t$, 10 runs



DOI: 10.1002/fld

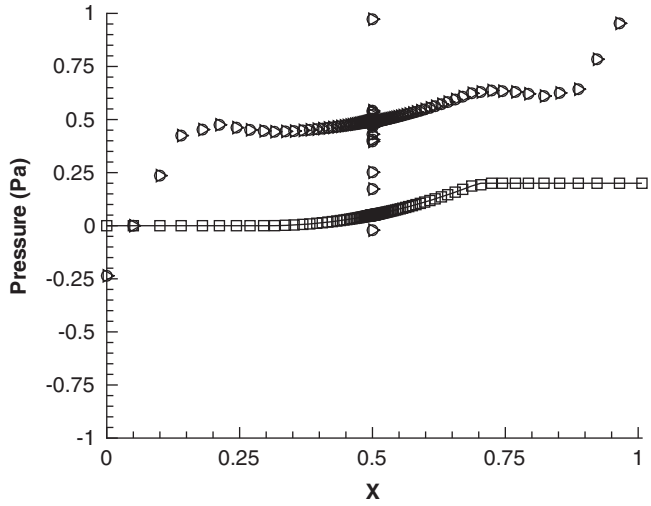


Figure 8. Pressure for the second case. ∘ PICTURETWO inconsistent $\Delta t = 10^{-4}$; ▷ PICTURETWO inconsistent $\Delta t = 10^{+5}$; □ PICTURETWO consistent $\Delta t = 10^{+5}$.

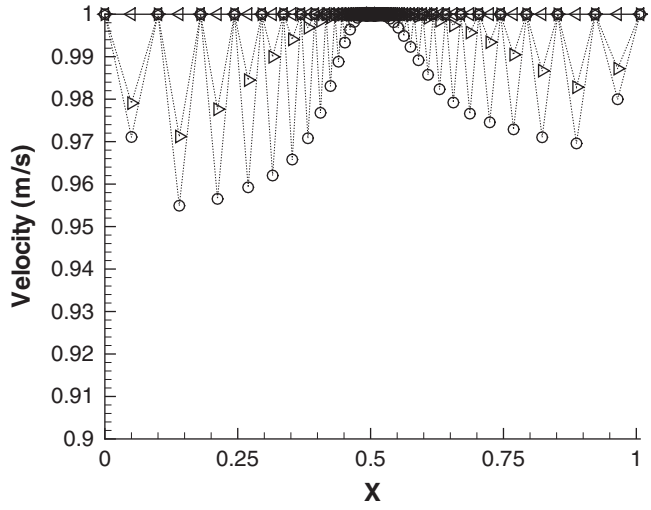


Figure 9. Velocity for the second case. ∘ Choi inconsistent $\Delta t = 10^{-4}$; ▷ Choi inconsistent $\Delta t = 10^{-3}$; ◁ Choi inconsistent $\Delta t = 10^{+5}$.

with $\Delta t$ ranging from $10^{-5}$ to $10^{2}$ in one order of magnitude intervals, plus $10^{5}$ and $10^{25}$, were carried out obtaining (bad) solutions differing only from the 12th decimal place onwards.

The velocity in this second case with Choi's scheme is presented in Figure 9. As there is no mass source the velocity solution at the cell interfaces has to be constantly equal to the inlet velocity, otherwise, the scheme would not conserve mass. It is well known that, unlike the face velocity, the cell velocity does not conserve mass in a colocated arrangement because the continuity equation is not applied to control volumes having the cell velocities on their faces. In fact these are calculated with their discretized transport equation. Owing to the wrong coupling between faces and nodes the results show a velocity field quite spiky. This is a clear example of a very simple flow in which both pressure and velocity behave erratically owing to the inconsistencies of the transient formulation.

In the course of this work we came across several unexpected oscillatory solutions of the consistent UNDS. One of them was the first test case, discussed and explained before, another is next one. This third computational case will allow us to compare the different alternatives one has



DOI: 10.1002/fld

for the evaluation of some of the terms at the cell interface of the consistent schemes. No matter how we evaluate $\delta_e$ for PICTURE the steady-state result is the same, but it is not so for UNDS. For the latter it is important to caution against an arbitrary evaluation of the factors associated with the cell face because if they are not computed properly the solution, otherwise smooth, can present some oscillations. In UNDS we have to look for interpolations that satisfy at steady state

$$A^u_{P|e}(1+\delta_e)-A^u_{P|e}\delta_e=\widetilde{A}^u_{P|e}-\frac{\rho_e\Delta V_e}{\Delta t}=A^u_{P|e} \tag{48}$$

As odd as it seems not all interpolations satisfy this trivial equality. For instance, if we used

$$\widetilde{A}^u_{P|e}=\overline{\widetilde{A}^u_{P|i}}^e=\overline{A^u_{P|i}}^e+\frac{\overline{\rho_i\Delta V_i}^e}{\Delta t} \quad \text{and} \quad \rho_e\Delta V_e=\widetilde{f}_x(\Delta M_P+\Delta M_E) \tag{49}$$

this interpolation would result in the following steady-state expression:

$$\left(\overline{A^u_{P|i}}^e+\frac{\overline{\rho_i\Delta V_i}^e}{\Delta t}-\frac{\rho_e\Delta V_e}{\Delta t}\right)u^*_e=\overline{A^u_{P|i}u^*_i}^e+\left[\overline{\Delta V_i\left.\frac{\partial p}{\partial x}\right|_i^l}^e-\Delta V_e\left.\frac{\partial p}{\partial x}\right|_e^l\right] \tag{50}$$

The problem arises if we use a nonuniform grid and $\Delta V_e$ is calculated in a mass-consistent way as $\rho_e\Delta V_e=\widetilde{f}_x(\Delta M_P+\Delta M_E)$. In that case the second and third terms in the LHS would not compensate each other and its difference would give rise to a non-unique steady-state solution dependent on the time step. Yet for a transient flow in a colocated grid this is the usual approach with UNDS-like schemes. For instance, Yu *et al.* [24] and some other researchers interpolate $\widetilde{A}^u_{P|e}$ and use a mass-consistent evaluation of $\Delta V_e$, this may sometimes produce oscillations and time step-dependent solutions. To corroborate this analysis let us choose an extremely simple flow: a constant velocity field with a constant momentum source of value one hundred between 0.3 and 0.7. The momentum source makes the pressure gradient to be constant in that interval. We will use a grid similar to that of the first test case. The results of pressure are portrayed in Figure 10 and those of velocity in Figure 11. For the oscillations to appear the difference between $\overline{\rho_i\Delta V_i}^e$ and $\rho_e\Delta V_e$, both divided by $\Delta t$, has to be comparable to $\overline{A^u_{P|i}}^e$ (i.e. the differential $\delta_e$ of order one), this requires a relatively small time step and a strong nonuniform grid. The results are shown for $\Delta t=5\times10^{-7}$ and $10^{-6}$. For this latter time step the interpolation that cancels out the difference is also shown. Two aspects stand out: the solution dependency on the time step and the disappearance of the oscillations when a mass-inconsistent interpolation is employed. As commented previously

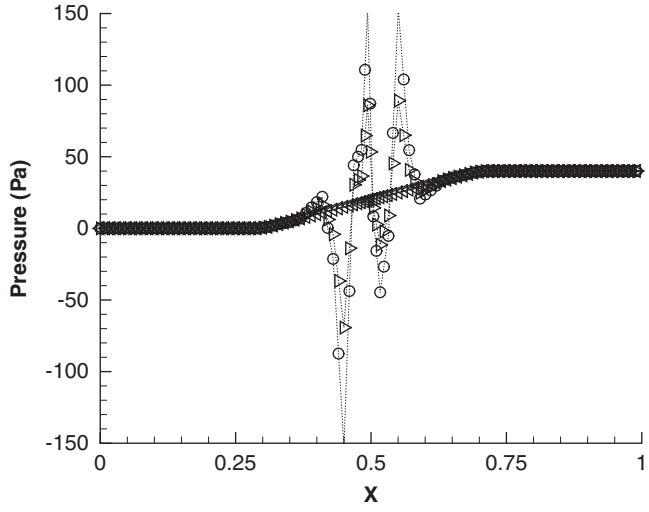


Figure 10. Pressure for the third case. ∘ UNDS mass-consistent $\Delta t=5.\ 10^{-7}$; ▷ UNDS mass-consistent $\Delta t=10^{-6}$; ◁ UNDS $\Delta V_e=\overline{\Delta V_i}^e$, $\Delta t=10^{-6}$.



DOI: 10.1002/fld

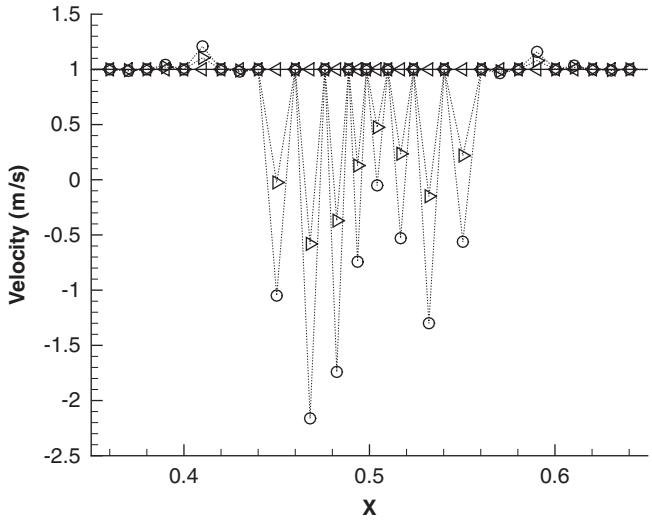


Figure 11. Velocity for the third case. ∘ UNDS mass-consistent $\Delta t = 5.\ 10^{-7}$; ▷ UNDS mass-consistent $\Delta t = 10^{-6}$; ◁ UNDS $\Delta V_e = \overline{\Delta V_i}^e$, $\Delta t = 10^{-6}$.

we have sometimes to abandon the idea of $\Delta V_e$ being a 'real' volume size. Because of the possibility of UNDS to produce oscillations it is not recommended for general use. We recognize that this last inconsistency encountered is very subtle, we came across it by sheer coincidence on using very small time steps. In any event, there is an alternative free of inconsistencies: PICTURE.

## 8. CONCLUSIONS

In this paper a thorough review of different proposals presented in the literature that deal with the (pseudo)unsteady Navier–Stokes equations in a colocated grid has been accomplished. By doing so, a general criterion to ascertain if a given scheme will be free of erroneous dependencies has been put forward and under this criterion the inconsistencies of former schemes have been highlighted. A new unconditionally consistent scheme has been derived and compared with others of the same class. It can be considered as the logical extension to transient problems of the Rhie–Chow procedure. This consistent scheme always provides time-independent solutions, unlike other consistent schemes in the literature that sometimes result in oscillatory and time-dependent solutions. Finally, a new manner of turning inconsistent schemes into consistent ones by using special interpolation practices has been explained.

We hope to clarify a subject that to our understanding remained a bit obscure: the extension to (pseudo)time-dependent problems of the procedures peculiar to a colocated grid. In particular, the consistent evaluation of the (pseudo)time-dependent cell face velocity without introducing unreal dependencies.

## APPENDIX A: EXACT SOLUTIONS OF THE COMPUTATIONAL CASES

In the first computational case we have the (constant) mass and momentum sources active in the interval $(x_1, x_2)$ in a domain of unit length. The boundary conditions for velocity and pressure on the left boundary are $u = u_o$ and $p = p_o$. In the interval between 0 and $x_1$ there is no source present, hence, the solution is $u = \text{const.} = u_o$, $p = \text{const.} = p_o$. At $x = x_1$ there is a discontinuity in the $u$ derivative from 0 to $\dot{m}/\rho$. This can be represented mathematically with the Heaviside step function whose derivative is the delta function. That means that at $x = x_1$ the viscous term becomes $(\dot{m}\mu/\rho)\delta(x - x_1)$. This delta function has to be compensated by the pressure gradient



DOI: 10.1002/fld

and consequently the pressure must also be a step function of amplitude $\dot{m}\mu/\rho$, that is, $p(x_1^+)=p_o+\dot{m}\mu/\rho$. In the interval where both sources are present the solution is

$$\begin{aligned} u(x) &= u_o+\frac{\dot{m}}{\rho}(x-x_1) \\ p(x) &= p_o+\frac{\dot{m}\mu}{\rho}+(S_m-\dot{m}u_o)(x-x_1)-\frac{\dot{m}^2}{2\rho}(x-x_1)^2 \end{aligned} \tag{A1}$$

At $x=x_2$ there is another delta function coming from the viscous term, hence, there is a new (negative) step in the pressure of the same amplitude. From $x=x_2$ onwards the solution is $p=p(x_2^+)$ and $u=u(x_2^+)$.

Summing up, the solution of the first computational case is

$$\begin{aligned} 0\leqslant x\leqslant x_1^- \quad & u(x)=u_o \;\; p(x)=p_o \\ x_1^+\leqslant x\leqslant x_2^- \quad & u(x)=u_o+\frac{\dot{m}}{\rho}(x-x_1) \\ & p(x)=p_o+\frac{\dot{m}\mu}{\rho}+(S_m-\dot{m}u_o)(x-x_1)-\frac{\dot{m}^2}{2\rho}(x-x_1)^2 \\ x_2^+\leqslant x\leqslant 1. \quad & u(x)=u_o+\frac{\dot{m}}{\rho}(x_2-x_1) \\ & p(x)=p_o+(S_m-\dot{m}u_o)(x_2-x_1)-\frac{\dot{m}^2}{2\rho}(x_2-x_1)^2 \end{aligned} \tag{A2}$$

The particular values of the variables employed in the first computational case are

$$\dot{m}=S_m=u_o=\rho=\mu=1, \quad p_o=0; x_1=0.3, \;\; x_2=0.7 \tag{A3}$$

The second case involves only a linear momentum source, $S_m=S_{mo}(x-x_1)/(x_2-x_1)$, active between $x_1$ and $x_2$. This source distribution produces a quadratic dependence for the pressure in that interval, this variable being continuous over the domain because there is no mass source. The velocity and pressure solutions are

$$\begin{aligned} 0\leqslant x\leqslant 1 \quad & u(x)=u_o \\ 0\leqslant x\leqslant x_1 \quad & p(x)=p_o \\ x_1\leqslant x\leqslant x_2 \quad & p(x)=p_o+\frac{S_{mo}}{2}\frac{(x-x_1)^2}{x_2-x_1} \\ x_2\leqslant x \quad & p(x)=p_o+\frac{S_{mo}}{2}(x_2-x_1) \end{aligned} \tag{A4}$$

The particular values of the variables employed in the second computational case are

$$S_{mo}=u_o=\rho=\mu=1, \quad \dot{m}=p_o=0, \quad x_1=0.3, \;\; x_2=0.7 \tag{A5}$$

ACKNOWLEDGEMENTS

The author wants to thank the Regional Government of Aragón for the IRDI agreement with the University of Zaragoza that allowed him to reduce the number of teaching hours and promoted his research activities.

REFERENCES

1. Rhie CM, Chow WL. Numerical study of the turbulent flow past an airfoil with trailing edge separation. *AIAA Journal* 1983; **21**(11):1525–1532.
2. Majumdar S. Role of underrelaxation in momentum interpolation for calculations of flows with nonstaggered grids. *Numerical Heat Transfer* 1988; **13**:125–132.



DOI: 10.1002/fld

3. Miller TF, Schmidt FW. Use of a pressure-weighted interpolation method for the solution of the incompressible Navier–Stokes equations on a nonstaggered grid system. *Numerical Heat Transfer* 1988; **14**:213–233.
4. Thiart GD. Finite difference scheme for the numerical solution of fluid flow and heat transfer problems on nonstaggered grids. *Numerical Heat Transfer Part B* 1990; **17**:43–62.
5. Wang GW, Wei JG, Tao WQ. An improved numerical algorithm for solution of convective heat transfer problems on nonstaggered grid system. *Heat and Mass Transfer* 1998; **33**:273–280.
6. Aksoy H, Chen CS. Numerical solution of Navier–Stokes equations with nonstaggered grids using finite analytic method. *Numerical Heat Transfer Part B* 1992; **21**:287–306.
7. Miettinen A. A study of the pressure correction approach in the colocated grid arrangement. *Lic. Thesis*, Helsinki University of Technology, 1997.
8. Date AW. Complete pressure correction algorithm for solution of incompressible Navier–Stokes equations on a nonstaggered grid. *Numerical Heat Transfer Part B* 1996; **29**:441–458.
9. Date AW. Solution of Navier–Stokes equations on nonstaggered grid. *International Journal of Heat and Mass Transfer* 1993; **36**:1913–1922.
10. Kobayashi MH, Pereira JCF. Numerical comparison of momentum interpolation methods and pressure–velocity algorithms using non-staggered grids. *Communications in Applied Numerical Methods* 1991; **7**:173–186.
11. Xu H, Zhang C. Study of the effect of the non-orthogonality for non-staggered grids—the theory. *International Journal for Numerical Methods in Fluids* 1998; **28**(9):1265–1280.
12. Kadja M, Anagnostopoulos JS, Bergeles GC. Study of wind flow and pollutant dispersion by newly developed precision-improving methods. *International Communications in Heat and Mass Transfer* 1996; **23**(8):1065–1076.
13. Kadja M, Anagnostopoulos JS, Bergeles GC. Implementation of newly developed algorithms in the simulation of atmospheric turbulent transports. *Computers and Fluids* 1997; **26**(5):489–504.
14. Yu B, Tao WQ, Wei JJ. Discussion on momentum interpolation method for colocated grids of incompressible flow. *Numerical Heat Transfer Part B* 2002; **42**:141–166.
15. Barton IE, Kirby R. Finite difference scheme for the solution of fluid flow problems on non-staggered grids. *International Journal for Numerical Methods in Fluids* 2000; **33**:939–959.
16. Johansson P, Davidson L. Modified collocated SIMPLEC algorithm applied to buoyancy-affected turbulent flow using a multigrid solution procedure. *Numerical Heat Transfer Part B* 1995; **28**:39–57.
17. Bohm M, Weschler K, Schafer M. A parallel moving grid multigrid method for flow simulation in rotor-stator configurations. *International Journal for Numerical Methods in Engineering* 1998; **42**:175–189.
18. Ferziger JH, Peric M. *Computational Methods for Fluid Dynamics* (2nd edn). Springer: Berlin, 1997.
19. Darwish M, Sraj I, Moukalled F. A coupled incompressible flow solver on structured grids. *Numerical Heat Transfer Part B* 2007; **52**:353–371.
20. Nilsson H, Davidson L. CALC-PVM: a parallel SIMPLEC multiblock solver for turbulent flow in complex domains. *Internal Report Nr 98/12*, Chalmers University of Technology, 1998.
21. Choi SK. Note on the use of momentum interpolation method for unsteady flows. *Numerical Heat Transfer Part A* 1999; **36**:545–550.
22. Lai YG, So RMC, Prezkwas AJ. Turbulent transonic flow simulation using a pressure-based method. *International Journal of Engineering Science* 1995; **33**(4):469–483.
23. Cubero A, Fueyo N. A compact momentum interpolation procedure for unsteady flows and relaxation. *Numerical Heat Transfer Part B* 2007; **52**:507–529.
24. Yu B, Kawaguchi Y, Tao WQ, Ozoe H. Checkerboard pressure predictions due to the underrelaxation factor and time step size for a nonstaggered grid with momentum interpolation method. *Numerical Heat Transfer Part B* 2002; **41**(1):85–94.
25. Lien FS, Leschziner MA. A general non-orthogonal collocated finite volume algorithm for turbulent flow at all speeds incorporating second-moment turbulence transport closure, part 1: computational implementation. *Computer Methods in Applied Mechanics and Engineering* 1994; **114**:123–148.
26. Udaykumar HS, Kan H-Ch, Shyy W, Tran-Son-Tay R. Multiphase dynamics in arbitrary geometries on fixed cartesian grids. *Journal of Computational Physics* 1997; **137**:366–405.
27. Gu CY. Computation of flows with large body forces. In *Numerical Methods in Laminar and Turbulent Flow*, Taylor C, Chin JH, Homsy GM (eds). Pineridge Press: Swansea, 1991; **7**(2):1568–1578.
28. Choi S-K, Kim S-O, Kim Ch-H, Choi H-K. Use of the momentum interpolation method for flows with a large body force. *Numerical Heat Transfer Part B* 2003; **43**:267–287.
29. Rahman MM, Miettinen A, Siikonen T. Modified SIMPLE formulation on a collocated grid with an assessment of the simplified QUICK scheme. *Numerical Heat Transfer Part B* 1996; **30**:291–314.
30. Mencinger J, Žun I. On the finite volume discretization of discontinuous body force field on collocated grid: application to VOF method. *Journal of Computational Physics* 2007; **221**:524–538.
31. Shen WZ, Michelsen JA, Sorensen JN. Improved Rhie–Chow interpolation for unsteady flow computations. *AIAA Journal* 2001; **39**(12):2406–2409.
32. Shen WZ, Michelsen JA, Sorensen NN, Sorensen JN. An improved SIMPLEC method on collocated grids for steady and unsteady flow computations. *Numerical Heat Transfer Part B* 2003; **43**:221–239.
33. Date AW. On interpolation of cell-face velocities in the solution of N-S equations using nonstaggered grids. *Report SFB 210/T/79*, University of Karlsruhe, 1991.



DOI: 10.1002/fld